European Journal of Remote Sensing - 2015, 48: 365-382
doi: 10.5721/EuJRS20154821
Received 12/03/2015, accepted 29/06/2015

European Journal of Remote Sensing
An official journal of the Italian Society of Remote Sensing

www.aitjournal.com

Delineation of Individual Tree Crowns from ALS and Hyperspectral data: a comparison among four methods

Michele Dalponte[1]*, Francesco Reyes[1], Kaja Kandare[2] and Damiano Gianelle[1,2]

[1]Department of Sustainable Agro-ecosystems and Bioresources, Research and Innovation Centre, Fondazione E. Mach, Via E. Mach 1, 38010 San Michele all'Adige (TN), Italy
[2]FoxLab, Joint CNR-FEM Initiative, Research and Innovation Centre, Fondazione E. Mach, Via E. Mach 1, 38010 San Michele all'Adige (TN), Italy
*Corresponding author, e-mail address: michele.dalponte@fmach.it

Abstract
In this paper four different delineation methods based on airborne laser scanning (ALS) and hyperspectral data are compared over a forest area in the Italian Alps. The comparison was carried out in terms of detected trees, while the ALS based methods are compared also in terms of attributes estimated (e.g. height). From the experimental results emerged that ALS methods outperformed hyperspectral one in terms of tree detection rate in two of three cases. The best results were achieved with a method based on region growing on an ALS image, and by one based on clustering of raw ALS point cloud. Regarding the estimates of the tree attributes all the ALS methods provided good results with very high accuracies when considering only big trees.

Keywords: Individual tree crowns delineation, biomass estimation, airborne laser scanning data, hyperspectral data.

Introduction
Forest ecosystems cover about 30% of our planet, account for 75% of the gross primary productivity of the Earth's biosphere, and contain 80% of the Earth's plant biomass [Pan et al., 2013]. Thus, they are very important for several reasons, both economical and environmental. Economically, forests are valuable as wood is a resource used in many fields, from buildings construction to energy generation. Environmentally, forests are very important as they preserve a great ecological diversity, for their protective role against natural hazards, and moreover as they represent a huge carbon sink, containing the majority of the carbon stored in terrestrial ecosystems [IPCC, 2000]. Indeed world's forests account for 50% of the annual carbon flux between the atmosphere and the Earth's land surface [Beer et al., 2010], and they capture and conserve more carbon than all other terrestrial ecosystems. The carbon is stored both in the form of biomass (trunks, branches, foliage, roots, etc.) and in the form of organic carbon in the soil [Carvalhais et al., 2014].
Regarding the carbon stored in form of biomass, a way to estimate it is through forest

inventories [Coomes et al., 2002]. Forest inventories can be carried out in several ways and there is not a standardized procedure used in all countries and regions. Forest inventories are usually based on the measurement of some field plots (e.g. one plot per hectare of forest) either of fixed size or using the angle count sampling technique [Gasparini and Di Cosmo, 2015; Piqué et al., 2011], and to average the values measured over stands having uniform structural characteristics [Gregoire and Valentine, 2008]. As usual for the surveys based on statistical sampling, which are preferred for large scale inventories to reduce the fieldwork, the spatial detail is not preserved, which can be problematic especially in forests managed with selective lodging, and characterized by the presence of mixed tree species.
In this context, remote sensing data are used in order to have more precise forest inventories without increasing the costs [Grafström and Ringvall, 2013]. Indeed remote sensing devices can provide objective information over large areas and, thanks to the most recent sensors, also a very high level of spatial detail of the estimated information. Almost all the remote sensing data available on the market can be used for the estimation of forest biomass and attributes [Anderson et al., 2008; Mette et al., 2002; Muukkonen and Heiskanen, 2005; Næsset, 2011]. Among all of them in the recent years great attention have been devoted to the use of airborne laser scanning (ALS) data for the estimation of structural properties of forests (e.g. above ground biomass) [Maltamo et al., 2014], while for qualitative parameters (e.g. tree species) hyperspectral data showed to be very effective [Dalponte et al., 2009a]. In particular, ALS data provide detailed information of the forest structure allowing to have precise estimations of biomass and volume [Bouvier et al., 2015]; hyperspectral data, with a dense sampling of the land covers spectral signatures, allow the detection of spectrally similar land covers (e.g. different tree species) [Dalponte et al., 2012; Tochon et al., 2015].
A forest inventory based on remote sensing data can be usually carried out at two spatial levels (area and individual tree crown level), depending on the available data and on the spatial detail requested by the final user [Vastaranta et al., 2009; Yu et al., 2010]. Forest inventories at coarser scales estimate the attributes of interest for areas of a certain size (e.g. 400 m^2, area-based approach, ABA), while in individual tree crowns (ITC) level inventories the attributes (including AGB) are estimated for each single tree detected in the study area. Obviously, the level of detail of the ITC level inventories is much higher, but obtained results are strongly dependent on the method used for the ITC delineation.
Many algorithms exist, each one with different characteristics and based on different input data. In the past the attention was mainly devoted to methods having raster images as input [Hyyppä et al., 2001; Popescu et al., 2003], mainly high resolution aerial images or canopy height models derived from ALS data [Ferraz et al., 2012]. Most recently, studies are focusing more and more on the use of the ALS point cloud in order to have a 3D representation of single trees, and to detect also suppressed trees and understory [Kandare et al., 2014]. Considering the effectiveness of different ITCs delineation methods, some comparative studies were recently published showing that, depending on the forest type, one method can be better than another [Eysn et al., 2015; Vauhkonen et al., 2012].
In this paper, a comparison of four ITC delineation methods, based on different data inputs and different algorithms, is presented. In particular the comparison aims at:

i. understanding which is the best delineation method to apply in a temperate forest, both in terms of delineation results and real applicability (e.g. computing time);
ii. understanding which is the best method in terms of tree attributes estimation for the

delineated ITCs (i.e. height, diameter at breast height, and above ground biomass);

iii. understanding if hyperspectral data can be used as replacement of ALS data for ITC delineation.

Data set description

Study area

The study area is a temperate forest located in the Italian Alps, in the municipality of Lavarone (Province of Trento, Italy), at an altitude of about 1350 m above sea level. The dominant tree species are Norway spruce (*Picea abies* (L.) Karst.), Silver fir (*Abies alba* Mill.) and European beech (*Fagus sylvatica* L.), with a tree volume composition of 64%, 34% and 2%, respectively. The area is of an uneven aged forest, with the oldest trees of about 130 years, as the management is not based on a real rotation plan but on partial cuttings of groups of about 10 tall trees, approximately every 10 years (Fig. 1). Average canopy height is 28 m, mean diameter at breast height (DBH) is 36 cm, and stem density is 401 trees/ha (DBH > 17.5 cm) and 1000 trees/ha (DBH in the range 7.5 - 17.5 cm), with a leaf area index (LAI) of 8.1 m^2 m^{-2}.

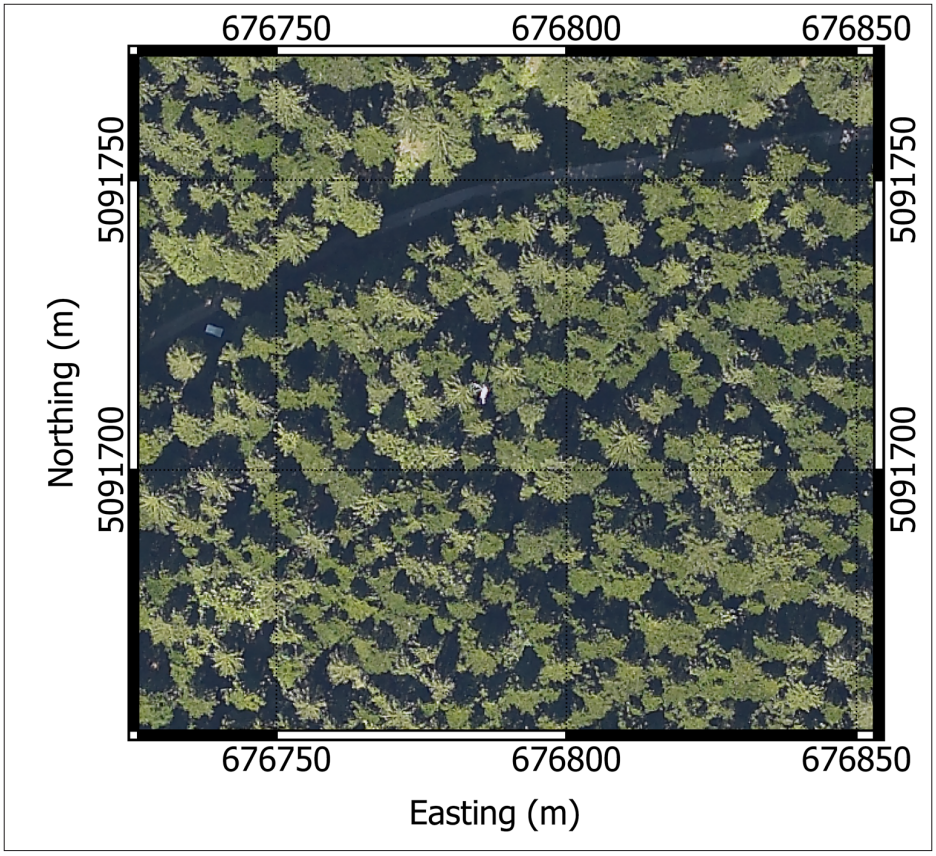

Figure 1 - Aerial image of the study area.

Remote sensing data description and preprocessing

ALS data were acquired on 8th of July 2011 with an Optech ALTM 3100EA sensor, with a mean point density of 8.6 points/m^2 for the first return (laser pulse wavelength 1064 nm, laser repetition rate 100 kHz) and with up to four recorded returns for each laser pulse. The data vendor generated a digital terrain model (DTM) starting from the acquired ALS data. The spatial resolution of the DTM was of 1 m.

Airborne hyperspectral data were acquired simultaneously to the ALS data with an AISA Eagle II sensor. 130 spectral bands equally spaced between 400 nm and 990 nm characterize the acquired image. The spatial resolution of the image is of 0.9 m.

The DTM value was subtracted from each ALS point, obtaining a normalized point cloud. The DTM was provided by the data vendor. A raster canopy height model (CHM) with 0.5 m spatial resolution was created from the ALS data. The CHM was obtained using the 99th percentile of the normalized Z values inside each pixel, and using a nearest neighbor interpolation. The hyperspectral images were resampled at 0.5 m spatial resolution in order to have the same resolution of the CHM used as input to delineation methods 1 and 2. The resampling was carried out with the commercial software ENVI (© 2015 Exelis Visual Information Solutions).

Field data

630 trees were inventoried in a plot of 4800 m^2, of which 58% Silver fir (basal area: 37 m^2/ha), 23% European beech (basal area: 2 m^2/ha), 19% Norway Spruce (basal area: 22 m^2/ha). For each tree with DBH higher than 1 cm in the study area DBH, position and species were recorded (Tab. 1). The position was defined respect to a based station using a Criterion Laser 400. The base station coordinates were collected using a differential GPS. The height and the above ground biomass (AGB) were estimated using the equations of Scrinzi et al. [2010].

Field data were matched with the delineated ITC according to the following procedure: if only one field measured tree was included inside an ITC then that tree was associated to that ITC. In the case of more than one field-measured tree was included in a segmented ITC, the field measured tree with the closer height to the ITC height was chosen.

Table 1 - Summary of the field measured trees.

DBH class (cm)	Number of trees			
	Total	*Picea abies* (L.) Karst.	*Abies alba* Mill.	*Fagus sylvatica* L.
< 7.5	236	14	105	117
7.5 - 17.5	136	29	88	19
17.5 - 27.5	79	15	57	7
27.5 - 47.5	126	35	89	2
> 47.5	53	24	27	2

Methods

ITC delineation methods

Method 1

Method 1 is based on the algorithm of Ene et al. [2012] and exploits both a CHM in raster format and the ALS point cloud with normalized z. The ITCs are firstly defined on the raster CHM using a watershed method and then they are reshaped using the normalized point cloud. In greater detail the steps of the method are the following:

1. a low-pass filter (LPF) is applied to the raster image of the CHM;
2. a watershed segmentation is applied to the filtered image, obtaining the image *L* of the segmented regions;
3. from each region in *L* the first return ALS points are extracted, and the Otsu thresholding method [Otsu, 1979] is applied to their normalized heights;
4. the first return ALS points higher than the Otsu threshold are extracted and a 2D convex hull is applied to these points;
5. the resulting polygons are the final ITCs.

In the results showed in this paper we used a LPF of 5x5 pixels size.

Method 2

Method 2 is based on the algorithm of Hyyppä et al. [2001] and exploits both a CHM in raster format and the ALS point cloud with normalized *z*. The ITCs are firstly defined on the raster CHM using a region growing method and then they are reshaped using the normalized point cloud. In greater detail the steps of the method are the following:

1. a LPF is applied to the raster image of the CHM;
2. seeds points $S = \{s_1,\ldots,s_N\}$ are defined using a moving window. A CHM pixel *CHM(x, y)* is a seed point if:

$$CHM(x,y) \in S \; if \begin{cases} CHM(x,y) = \max(moving\ window) \\ CHM(x,y) > h_{TH} \end{cases} \quad [1]$$

where h_{TH} is a minimum height threshold fixed by the user;

3. initial regions are defined starting from the seed points. A label map *L* is defined:

$$\begin{cases} L_{i,j} = k \; if \; CHM(i,j) \in S \\ L_{i,j} = 0 \; if \; CHM(i,j) \notin S \end{cases} \quad [2]$$

4.starting from the seed points regions grow according to the following procedure:

   a. consider a label map point $L_{i,j} \neq 0$ and take its neighbor pixels (*NP*) in the CHM:

$$NP = \{CHM(i,j-1);\mathrm{CHM}(i-1,j);\mathrm{CHM}(i,j+1);\mathrm{CHM}(i+1,j)\} \quad [3]$$

   b. a neighbor pixel $NP(i',j')$ is added to the region *n* if:

$$\begin{cases} dist\left(NP\left(i^{'},j^{'}\right),s_n\right) < DistMax \\ NP\left(i^{'},j^{'}\right) > \left(s_n * PercThresh\right) \\ L_{i^{'},j^{'}} \neq 0 \end{cases} \quad [4]$$

where $PercThresh \in (0;1)$, $DistMax > 0$, and s_n is the seed point of the region n. If these conditions are satisfied the value in the label map L corresponding to the pixel $NP\left(i^{'},j^{'}\right)$ is set to n: $L_{i^{'},j^{'}} = n$.

c. the steps a) and b) are iterated over all the pixels that have $L_{i,j} \neq 0$, and it is repeated until no pixels are added to any region;

5. from each region in *L* the first return ALS points are extracted and Otsu thresholding is applied [Otsu, 1979] to their normalized heights;
6. the first return ALS points higher than the Otsu threshold are extracted and a 2D convex hull is applied to these points;
7. the resulting polygons are the final ITCs.

In the results showed in this paper we used a LPF of 5x5 pixels size, a value of *PercThresh* of 0.7, and of *DistMax* of 10 pixels.

Method 3

Method 3 is the method presented in Kandare et al. [2014]. The input of this method is a normalized ALS point cloud, defined with X, Y and Z coordinates. This method is based on clustering of the ALS point cloud. The main steps of the method are detailed below:

1. the normalized point cloud is divided into vertical layers along the *Z* axis, considering only points above 1.5 m to remove effects of terrain objects, shrubs and herbaceous vegetation. The vertical layers have a distance fixed by the user;
2. 3D K-means clustering is applied to the normalized points of the point cloud in each layer and barycenters (BCs) are calculated for each 3D K-means cluster;
3. starting from the BCs, the 3D K-means clusters are aggregated. A 3D ellipsoid is created from the top BC (located in the North Pole of the ellipsoid). Then, all the clusters that have a corresponding BC inside the ellipsoid are aggregated. The size of the ellipsoid (minor and major axis) is tuned on the basis of the *Z* coordinate of the BC (higher *Z* values lead to bigger ellipsoids);
4. a Kernel density function is applied to the 3D clusters in order to estimate the distribution of the normalized ALS point cloud points along *X* and *Y* axes. Uneven distributed points are separated into two new 3D clusters depending on the presence of a gap bigger than a predefined threshold (computed as a mean distances between *X* and *Y* values of the ALS points) between the points;
5. 3D clusters with the same index within different layers are merged along the vertical direction. The merging procedure is carried out defining 2D polygons along the horizontal direction of the 3D clusters. Polygons with the same index are sorted by height in descending order. Starting from the top polygon, clusters with overlapping polygons for more than 10% are merged. If not, the cluster is reindexed;

6. a Kernel density function is applied to the unique 3D clusters along the *Z* direction. Uneven distributed points inside the clusters are separated into two 3D clusters if there is a gap between points bigger than a given threshold;
7. unique 3D clusters are merged together along the vertical direction. The merging criteria used in this step is the same as in step 5;
8. in order to refine the preliminary result, some small remaining clusters need to be merged to a bigger cluster or deleted. These "outlaying" clusters are selected if they deviate from the average mean crown area, number of points within the cluster, cluster height or height range of the ALS points inside the cluster. The selected outlaying clusters are merged to a bigger cluster if the following condition is fulfilled. The merging procedure is carried out defining 2D polygons (see part 5) which are merged them along the vertical direction. Starting from the top polygon, the clusters are compared to the outlaying ones and reshaped if their polygons overlap for 10%. Outlaying clusters that were not merged are removed if their cluster's projected area on the horizontal plane is smaller than minimal crown area threshold (obtained from the field data). Finally, the small clusters are merged to bigger clusters and grouped into final 3D clusters representing the ITCs;
9. 2D polygons are generated for each clusters using the convex hull method.

In the results showed in this study the number of layers of step 1 was fixed to 10 with the same amount of points within each layer, and the threshold of step 6 was fixed at 4 m.

Method 4

Method 4 is based on the use of hyperspectral data and it was developed *ad hoc* for this study following the structure of Method 2. In greater detail the steps of the method are the following:

1. a LPF is applied to one raster band selected among the bands of the hyperspectral image;
2. seeds points $S = \{s_1,\ldots,s_N\}$ are defined using a moving window. An image pixel *H(x,y)* is a seed point if:

$$H(x,y) \in S \; if \; H(x,y) = \max(moving\ window) \quad [5]$$

3. initial regions are defined starting from the seed points. A label map *L* is defined:

$$\begin{cases} L_{i,j} = k \; if \; H(i,j) \in S \\ L_{i,j} = 0 \; if \; H(i,j) \notin S \end{cases} \quad [6]$$

4. starting from the seed points regions grow according to the following procedure:
   a. consider a label map point and take its neighbor pixels (*NP*) in the image:

$$NP = \{H(i,j-1);\mathrm{H}(i-1,j);\mathrm{H}(i,j+1);\mathrm{H}(i+1,j)\} \quad [7]$$

b. a neighbor pixel $NP\left(i^{'},j^{'}\right)$ is added to the region *n* if:

$$\begin{cases} dist\left(NP\left(i^{'},j^{'}\right),s_n\right) < DistMax \\ NP\left(i^{'},j^{'}\right) > \left(s_n * PercThresh\right) \\ L_{i^{'},j^{'}} \neq 0 \end{cases} \quad [8]$$

where $PercThresh \in (0;1)$, $DistMax > 0$, and s_n is the seed point of the region *n*. If these conditions are satisfied the value in the label map L corresponding to the pixel $NP\left(i^{'},j^{'}\right)$ is set to *n*: $L_{i^{'},j^{'}} = n$.

c. the steps a) and b) are iterated over all the pixels that have $L_{i,j} \neq 0$, and it is repeated until no pixels are added to any region;

5. from each region in L the central coordinates of each pixel are extracted, and a 2D convex hull is applied to these points;
6. the resulting polygons are the final ITCs.

The raster image used in this paper was the image from the band at 810 nm, already used in previous studies for this purpose [Clark et al., 2005; Dalponte et al., 2014]. The LPF filter used had a dimension of 3x3 pixels, the moving window a size of 5x5 pixels, the value of *PercThresh* was of 0.7, and of *DistMax* of 10.

Estimation of ITC attributes

The height, DBH and AGB of each ITC, delineated using ALS data, were estimated using some variables extracted from ALS data as in Dalponte et al [2009b; 2011]. Among them, only the ones that showed to be significant predictors in a generalized linear regression model for the estimations of height, DBH and AGB were selected by means of the stepAIC function of the R [R Development Core Team, 2008] package MASS. The analysis of the results was done considering two DBH classes: i) DBH < 17.5 cm; and ii) DBH ≥ 17.5 cm. We chose 17.5 cm as a threshold as it is the normal threshold used in the Province of Trento to separate inventory and pre-inventory trees in a forest inventory. The results of the estimations over the commonly matched trees were compared using the Mann-Whitney-Wilcoxon test.

Results

ITC delineation

In Table 2 the quantitative results of the ITC delineation with the four methods considered is showed. Method 2 provided the highest detection rate (DET) for both DBH classes. Considering all the trees, the detection rate is quite low as only about one fourth of the trees were detected. However, when only trees with DBH higher than 17.5 cm were considered (the standard threshold used in Italy for the stem volume estimation), DET increased to 61%.

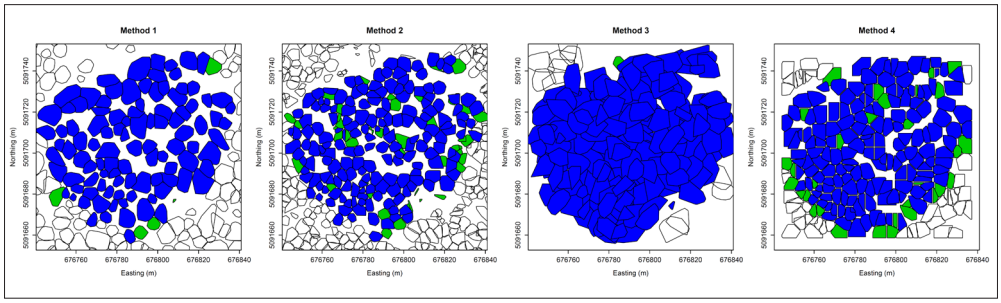

Figure 2 - Delineation results. The colored crowns are the ones inside the study area. The blue ones are the one matched with a field measurement, while the green ones are cases of commission errors.

Analyzing the other accuracy parameters it is possible to note that other methods reach better performances. Method 3 performs better when considering the accuracy index (AI). This index considers both omission (OE) and commission (CE) errors and, in fact, Method 3 obtained a very low CE. Differently, considering only the OE, Method 2 had the best results. Looking at the three tree species present in the area, it can be seen that for Norway spruce the best performances are reached with Method 2, for Silver fir with Method 2 and 3, while for European beech with method 2, 3, and 4.

Table 2 - Quantitative results of the ITC delineation for the four delineation methods considered. The best results are highlighted in bold.

Method	DBH (cm)	Number of field measured trees	Number of ITC matched	DET (%)				AI (%)	OE (%)	CE (%)
				Total	Picea abies	Abies alba	Fagus sylvatica			
1	all	630	102	16.2	20.5	19.4	4.8	11.5	83.8	4.7
	>17.5	258	100	38.8	32.4	41.0	45.5	32.3	61.2	6.5
2	all	630	**175**	**27.8**	**43.6**	**29.5**	10.9	7.0	**72.2**	20.8
	>17.5	258	**157**	**60.9**	**64.9**	57.8	**81.8**	31.8	**39.2**	29.0
3	all	630	155	24.6	28.2	28.1	12.9	**24.0**	75.4	**0.6**
	>17.5	258	140	54.3	40.5	**58.4**	**81.8**	**44.0**	45.7	**10.3**
4	all	630	157	24.9	18.8	23.5	**33.3**	8.4	75.1	16.5
	>17.5	258	127	49.2	33.8	53.8	**81.8**	16.7	50.8	32.5

Making a visual analysis of the ITCs (Fig. 2), it is clear that the ITCs of Method 3 covered all the area with a high degree of overlapping among polygons. Conversely, Method 1 and 2 left large spaces between the ITCs. Method 1 produced few ITCs, with gaps between them, thus increasing the omission error. In Method 4 shape and size of detected ITCs are clearly affected by the pixel size of the starting raster image.

ITC attributes estimation

Considering all the three estimated parameters (height, DBH and AGB), the best results were shown by Method 1 (Figs. 3, 4 and 5).

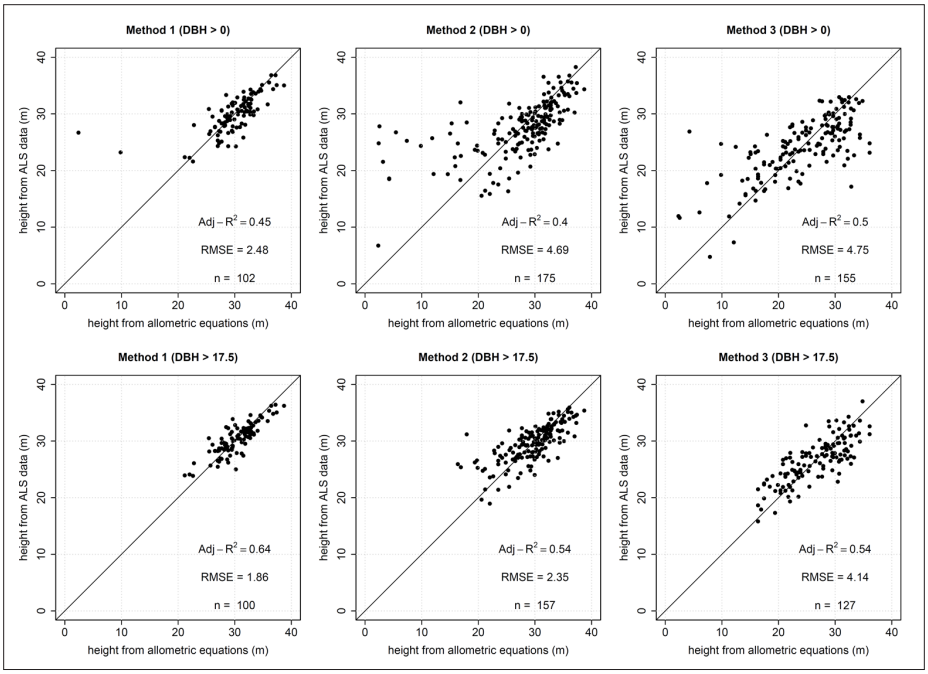

Figure 3 - Height estimation results with the three methods based on ALS data, considering two DBH classes.

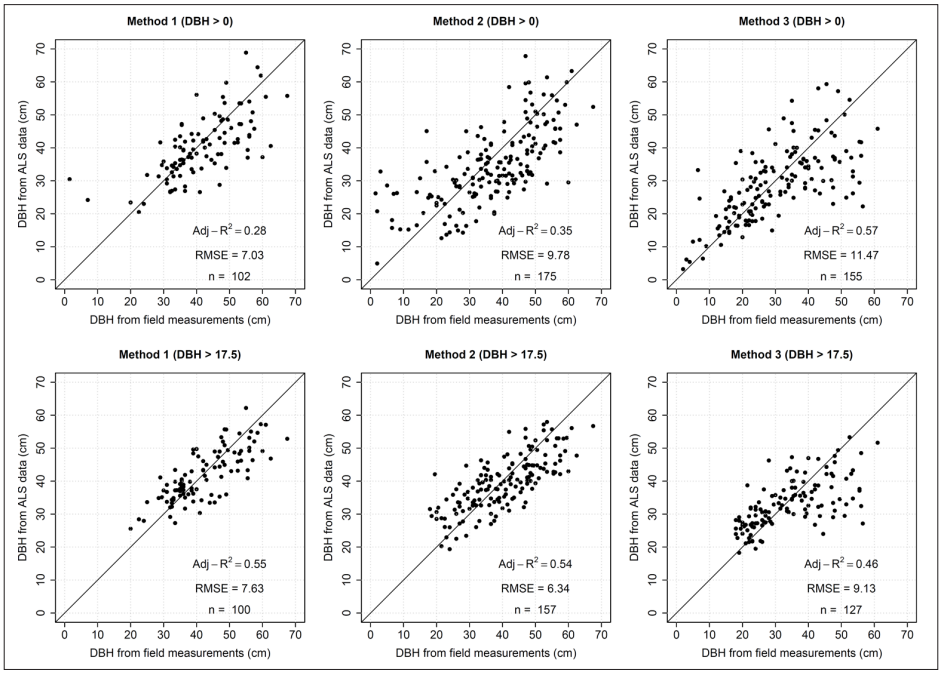

Figure 4 - DBH estimation results with the three methods based on ALS data, considering two DBH classes.

In each plot, the mean Adjusted-R^2 and the mean RMSE of the leave-one-out estimation are showed. These reached an Adjusted-R^2 of 0.64 and a RMSE of 1.86 m in the estimation of the tree heights, for the trees with DBH higher than 17.5 cm. All the methods largely overestimated the heights of the small trees. This is probably due to a matching problem among the field measured trees and the delineated ITCs. Method 3 provided the largest estimation errors. Comparing the height of the trees detected by all the three ALS based methods (49 trees), it can be seen that the estimates obtained by Method 1 and 2 have the highest correlation ($R^2 = 0.57$) while Methods 1 and 3 are the least correlated ($R^2 = 0.29$) (Tab. 3). In all the pairs (i.e. Method 1 vs Method 2, Method 1 vs. Method 3, and Method 2 vs. Method 3) it emerged that the estimates were statistically different at 0.05 significance level (Tab. 3).

Table 3 - Comparison among the estimation results of height, DBH, and AGB obtained from the ITCs delineated with the three delineation methods based on ALS. The p-value is obtained with the Mann-Whitney-Wilcoxon test.

Attribute	Comparison	R^2	RMSE	p-value
Height	Method 1 vs Method 2	0.57	2.54	0.018
	Method 1 vs Method 3	0.29	4.45	0.000
	Method 2 vs Method 3	0.32	3.55	0.002
DBH	Method 1 vs Method 2	0.74	4.06	0.291
	Method 1 vs Method 3	0.37	8.87	0.000
	Method 2 vs Method 3	0.36	7.53	0.000
AGB	Method 1 vs Method 2	0.70	232.3	0.961
	Method 1 vs Method 3	0.48	307.4	0.687
	Method 2 vs Method 3	0.53	224.2	0.676

The DBH was estimated with an RMSE lower than 10 cm, with the best result (6.29 cm) obtained by Method 2 and trees with DBH larger than 17.5 cm. Conversely, Method 3 provided the largest estimation errors (RMSE from 8.87 to 10.81). Adjusted-R^2s were quite low for all methods, with the highest values around 0.55, and the lowest around 0.28. In particular, the estimation of DBH was systematically overestimated by all the three methods. From Table 3 it can be seen that the DBHs estimated by Method 1 and 2 have the highest correlation ($R^2 = 0.74$) while Methods 2 and 3 are the least correlated ($R^2 = 0.36$). The DBHs estimated with Method 1 and Method 2 resulted not statistically different at 0.05 significance level, while the other pairs (i.e. Method 1 vs. Method 3, and Method 2 vs. Method 3) resulted to be statistically different at 0.05 significance level (Tab. 3).

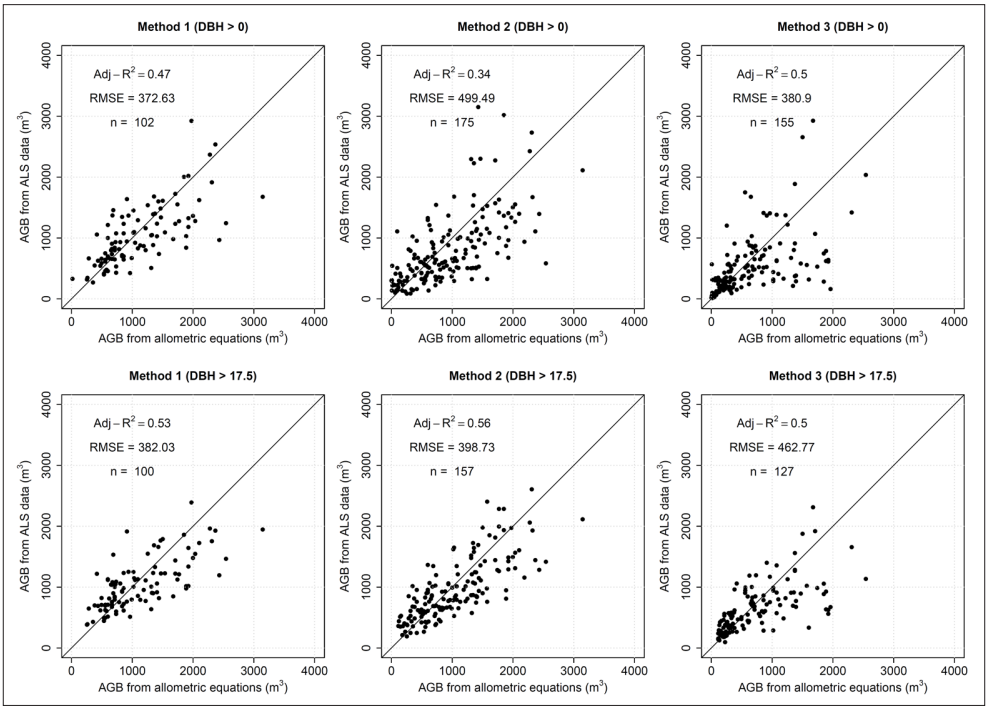

Figure 5 - AGB estimation results with the three methods based on ALS data, considering two DBH classes.

Analyzing the AGB estimations (Fig. 5) it is clear that there is a problem in the estimation of the large values of AGB. In this case the best results in terms of RMSE were obtained with Method 1 while in terms of Adjusted-R^2 by Method 2. Differently than from the height and DBHs, for AGB there is an underestimation of the largest values of AGB by all methods. From Table 3 it can be seen that the AGBs estimated by Method 1 and 2 have the highest correlation ($R^2 = 0.70$) while Methods 1 and 3 are the least correlated ($R^2 = 0.48$). In all the pairs (i.e. Method 1 vs. Method 2, Method 1 vs. Method 3, and Method 2 vs. Method 3) it emerged that the estimates were not statistically different at 0.05 significance level (Tab. 3).

Table 4 - Total AGB measured in the field and estimated by the three delineation methods based on ALS data.

DBH (cm)	Total AGB (kg)			
	Field	Method 1	Method 2	Method 3
All	232226	103742	137051	78800
> 17.5	232106	103627	149725	82386

In Table 4 the total AGB of the study area measured in the field and estimated by the three Methods is showed. It can be seen that, at best, about 60% of the total AGB was estimated, while in the worst case only about 34%. It is worth noting also that trees with DBH smaller than 17.5 cm accounts for a very little amount of the total AGB.

Discussion

The four delineation methods considered provided very different results and, depending on which accuracy statistic is considered, different methods are achieving the best performance. Looking only at the detection rate, Method 2 reached the best results while, considering the accuracy index (AI), Method 4 was the best one. This because Method 4 had very low commission errors. These results showed that it is not univocal how to define if a method is good or not, as it depends on the needs of the final user. Among the four methods analyzed here, it is clear that Method 2 have the tendency to over-segment the image. This leads, on one hand, to have a high detection rate but, on the other hand, to have a high commission error. Moreover, the delineated trees are not always representing the real size of the forest trees. On the opposite side, Method 3 defines much bigger segments that reduce at minimum the commission error, at the cost of a lower detection rate. Similarly, method 1 gives segments bigger than in Method 2 and, consequently, a lower commission error. Indeed, Method 1 had the lowest detection rate, but a higher accuracy index compared to Method 2 (that had the highest detection rate).

Considering the processing time Method 3 is about 10 times slower than the other three, while Method 4 is the fastest. This affect the practical application of the delineation methods in forest inventories. Method 2 is probably the one to be suggested to be used in real cases as it provides a good compromise among processing time and results obtained in terms of detected trees and estimation of the tree attributes. Moreover if the interest is only in locating the tree positions and to estimate the tree heights, the computing time of Method 2 can be reduced of about 10 times, making it usable also over large areas. In fact the crown delineation procedure is the most time consuming.

The results of this study are in line with the literature, especially considering only the inventory trees (DBH > 17.5 cm). Vauhkonen et al. [2012] in a comparative study of six delineation methods over different countries showed an average detection rate of 48% in coniferous and broadleaved forests (Germany), 42% and 60% in boreal forests of Norway and Sweden, respectively. Reitberger et al. [2009] in an alpine spruce forest, a mixed mountain forest and a spruce forest obtained a detection rate in a range from 48% to 60%. Regarding the height estimation, also in other studies emerged the fact that small heights are frequently overestimated [Hyyppä and Inkinen, 1999; Persson et al., 2002; Ferraz et al., 2012]. This may be due to the fact that the treetop is not necessarily sampled by the laser scanner.

Only a few trees were detected by all the four methods (9 field measured trees), as by the ALS based methods alone (49 trees). Every method is detecting different trees. The two methods that appears to be more consistent among each other are method 1 and 2, and this is showed also by the estimated parameters. In particular these two methods had similar results in terms of estimated height, DBH and AGB on the 49 trees cited above.

In the considered study area almost half of the trees belong to suppressed or understory layers and this obviously decreases the detection rate. This explains why all the methods achieved a very low detection rate considering all the trees, while the detection rate is much higher considering the big trees only. From a forestry viewpoint the big trees (DBH>17.5 cm) are the most important, as these are the trees valuable for their wood. However, from an ecological point of view it is important to study also the understory layers. Thus, a method that can detect also small trees is preferable.

Similar considerations can be made regarding the three tree species present in the area. The wood of Norway spruce and Silver fir is important from an economical viewpoint, as it is used for manufacturing purposes, while the wood of European beech is usually used for energy production (i.e. heating systems). Considering the carbon sinks, all species are important, and it is worth to have a good detection rate for all of them. From our results it is clear that all the species experienced similar detection results, even if there are slightly better results for the European beech.

The method based on hyperspectral data showed a good detection rate, similar to the one of ALS methods. This result is better than what was found in other studies in the literature [Dalponte et al., 2014]. One factor that may have influenced the results is the crown size of the trees. Comparing the average crown size of the trees in the dataset used in Dalponte et al. [2014] with the one of this study, it emerged that the trees in this study have larger crowns. In this regard Hengl [2006] suggested that having at least four pixels representing the smallest circular objects and at least two pixels representing the narrowest objects is crucial in order to detect an object in an image. Following this rule of thumb the spatial resolution of the imagery used for the delineation should match the expected minimum size of the tree crowns across the scene. Keeping constant the spatial resolution, if in a study area the trees are smaller than in another one, the detection rate will be lower. Consequently, ALS data result more flexible since their spatial resolution can be easily adjusted, while resolution in hyperspectral data is usually fixed at the time of the acquisition. Additionally, a main drawback in using hyperspectral data is that the estimation of height, DBH, and AGB is not straightforward as it is for ALS data. First of all there is a problem of saturation for the big trees, as the relationship among spectral variables and AGB saturates at a certain point [Lu, 2005]. Moreover, if a proper atmospheric correction is not carried out, the estimations will be strongly influenced by the conditions at the time of acquisition. In this regard, some studies exist that relates hyperspectral bands to these variables [Tonolli et al., 2011; Vaglio Laurin et al., 2014] but, as the data that we used were not atmospherically corrected, we preferred to not perform estimations for hyperspectral data. In any case the results achieved with these data are not comparable with ALS ones [Coops et al., 2004; Koch, 2010; Tonolli et al., 2011; Vaglio Laurin et al., 2014]. The delineation carried out with hyperspectral data can be very useful if the only objective is the classification of tree species. However, this is usually a rare task in forestry where the main interest is usually in quantitative variables (e.g., stem volume).

Conclusions

In this paper, four ITC delineation methods based on ALS and hyperspectral data have been compared. The results achieved showed that all the methods performed well and, according to the considered metric, the best results were achieved with a method based on region growing on a raster ALS image, and by a clustering method based on raw ALS point cloud. We suggest to use the method based on region growing in large areas inventories as it is about 10 times faster than the one based on ALS point cloud clustering. The hyperspectral based method gave results comparable to some ALS methods, showing that also hyperspectral data at very high geometrical resolution can be a good information source to use for ITCs delineation. All the ALS methods showed to be effective in the estimations of trees attributes. One limitation common to all the methods is that the suppressed and understory

trees are rarely detected, and even if this influence very little the total AGB of a forest, it can be problematic when other parameters are needed, like the diameters distribution of trees in a forest.

Acknowledgements

The work leading to this research was supported by the Trees4Future project co-funded by the European Union Seventh Framework Programme FP7 under grant agreement n° 284181 "Trees4Future".

References

Anderson J.E., Plourde L.C., Martin M.E., Braswell B.H., Smith M.L., Dubayah R.O., Hofton M.A., Blair J.B. (2008) - *Integrating waveform lidar with hyperspectral imagery for inventory of a northern temperate forest*. Remote Sensing of Environment, 112 (4): 1856-1870. doi: http://dx.doi.org/10.1016/j.rse.2007.09.009.

Beer C., Reichstein M., Tomelleri E., Ciais P., Jung M., Carvalhais N., Rödenbeck C., Arain M.A., Baldocchi D., Bonan G.B., Bondeau A., Cescatti A., Lasslop G., Lindroth A., Lomas M., Luyssaert S., Margolis H., Oleson K.W., Roupsard O., Veenendaal E., Viovy N., Williams C., Woodward F.I., Papale D. (2010) - *Terrestrial gross carbon dioxide uptake: global distribution and covariation with climate*. Science, 329 (5993): 834-838. doi: http://dx.doi.org/10.1126/science.1184984.

Bouvier M., Durrieu S., Fournier R., Renaud J. (2015) - *Generalizing predictive models of forest inventory attributes using an area-based approach with airborne LiDAR data*. Remote Sensing of Environment, 156: 322-334. doi: http://dx.doi.org/10.1016/j.rse.2014.10.004.

Carvalhais N., Forkel M., Khomik M., Bellarby J., Jung M., Migliavacca M., Mingquan M., Saatchi S., Santoro M., Thurner M., Weber U., Ahrens B., Beer C., Cescatti A., Randerson J.T., Reichstein M. (2014) - *Global covariation of carbon turnover times with climate in terrestrial ecosystems*. Nature, 514: 213-217. doi: http://dx.doi.org/10.1038/nature13731.

Clark M.L., Roberts D.A., Clark D.B. (2005) - *Hyperspectral discrimination of tropical rain forest tree species at leaf to crown scales*. Remote Sensing of Environment, 96: 375-398. doi: http://dx.doi.org/10.1016/j.rse.2005.03.009.

Coomes D.A., Allen R.B., Scott N.A., Goulding C., Beets P. (2002) - *Designing systems to monitor carbon stocks in forests and shrublands*. Forest Ecology and Management, 164 (1-3): 89-108. doi: http://dx.doi.org/10.1016/S0378-1127(01)00592-8.

Coops N.C., Wulder M.A., Culvenor D.S., St-Onge B. (2004) - *Comparison of forest attributes extracted from fine spatial resolution multispectral and lidar data*. Canadian Journal of Remote Sensing, 30 (6): 855-866. doi: http://dx.doi.org/10.5589/m04-045.

Dalponte M., Bruzzone L., Gianelle D. (2011) - *A system for the estimation of single-tree stem diameter and volume using multireturn LIDAR data*. IEEE Transaction on Geoscience and Remote Sensing, 49 (7): 2479-2490. doi: http://dx.doi.org/10.1109/TGRS.2011.2107744.

Dalponte M., Bruzzone L., Gianelle D. (2012) - *Tree species classification in the Southern Alps based on the fusion of very high geometrical resolution multispectral/hyperspectral images and LiDAR data*. Remote Sensing of Environment, 123: 258-270. doi: http://

dx.doi.org/10.1016/j.rse.2012.03.013.

Dalponte M., Bruzzone L., Vescovo L., Gianelle D. (2009a) - *The role of spectral resolution and classifier complexity in the analysis of hyperspectral images of forest areas*. Remote Sensing of Environment, 113: 2345-2355. doi: http://dx.doi.org/10.1016/j.rse.2009.06.013.

Dalponte M., Coops N.C., Bruzzone L., Gianelle D. (2009b) - *Analysis on the use of multiple returns LiDAR data for the estimation of tree stems volume.* IEEE Journal of Selected Topics in Applied Earth Observations and Remote Sensing, 2 (4): 310-318. doi: http://dx.doi.org/10.1109/JSTARS.2009.2037523.

Dalponte M., Ørka H.O., Ene L.T., Gobakken T., Næsset E. (2014) - *Tree crown delineation and tree species classification in boreal forests using hyperspectral and ALS data*. Remote Sensing of Environment, 140: 306-317. doi: http://dx.doi.org/10.1016/j.rse.2013.09.006.

Ene L., Næsset E., Gobakken T. (2012) - *Single tree detection in heterogeneous boreal forests using airborne laser scanning and area-based stem number estimates.* International Journal of Remote Sensing, 33 (16): 5171-5193. doi: http://dx.doi.org/10.1080/01431161.2012.657363.

Eysn L., Hollaus M., Lindberg E., Berger F., Monnet J.-M., Dalponte M., Kobal M., Pellegrini M., Lingua E., Mongus D., Pfeifer N. (2015) - *A Benchmark of Lidar-Based Single Tree Detection Methods Using Heterogeneous Forest Data from the Alpine Space*. Forests, 6: 1721-1747. doi: http://dx.doi.org/10.3390/f6051721.

Ferraz A., Bretar F., Jacquemoud S., Gonçalves G., Pereira L., Tomé M., Soares P. (2012) - *3-D mapping of a multi-layered Mediterranean forest using ALS data*. Remote Sensing of Environment, 121: 210-223. doi: http://dx.doi.org/10.1016/j.rse.2012.01.020.

Gasparini P., Di Cosmo L. (2015) - *Forest carbon in Italian forests: Stocks, inherent variability and predictability using NFI data*. Forestry Ecology and Management, 337: 186-195. doi: http://dx.doi.org/10.1016/j.foreco.2014.11.012.

Grafström A., Ringvall A.H. (2013) - *Improving forest field inventories by using remote sensing data in novel sampling designs*. Canadian Journal of Forest Research, 43: 1015-1022. doi: http://dx.doi.org/10.1139/cjfr-2013-0123.

Gregoire T.G., Valentine H. (2008) - *Sampling strategies for natural resources and the environment*. Chapman & Hall/CRC, Boca Raton, Florida, 496 pp.

Hengl T. (2006) - *Finding the right pixel size*. Computers & Geoscience, 32: 1283-1298. doi: http://dx.doi.org/10.1016/j.cageo.2005.11.008.

Hyyppä J., Inkinen M. (1999) - *Detecting and estimating attributes for single trees using laser scanner*. Photogrammetric Journal of Finland, 16: 27-42.

Hyyppä J., Kelle O., Lehikoinen M., Inkinen M. (2001) - *A segmentation-based method to retrieve stem volume estimates from 3-D tree height models produced by laser scanners*. IEEE Transaction on Geoscience and Remote Sensing, 39: 969-975. doi: http://dx.doi.org/10.1109/36.921414.

IPCC (2000) - *Land-use, land-use change, and forestry: A special report of the IPCC.* Cambridge University Press, Cambridge and New York.

Kandare K., Dalponte M., Gianelle D., Chan J.C. (2014) - *A new procedure for identifying single trees in understory layer using discrete LiDAR data.* IEEE Geoscience and Remote Sensing Symposium, Quebec City, pp. 1357-1360. doi: http://dx.doi.org/10.1109/

IGARSS.2014.6946686.

Koch B. (2010) - *Status and future of laser scanning, synthetic aperture radar and hyperspectral remote sensing data for forest biomass assessment*. ISPRS Journal of Photogrammetry and Remote Sensing, 65 (6): 581-590. doi: http://dx.doi.org/10.1016/j.isprsjprs.2010.09.001.

Lu D. (2005) - *Aboveground biomass estimation using Landsat TM data in the Brazilian Amazon*. International Journal of Remote Sensing, 26 (12): 2509-2525. doi: http://dx.doi.org/10.1080/01431160500142145.

Maltamo M., Naesset E., Vauhkonen J. (2014) - *Forestry Applications of Airborne Laser Scanning*. Springer. doi: http://dx.doi.org/10.1007/978-94-017-8663-8.

Mette T., Papathanassiou K.P., Hajnsek I., Zimmermann R. (2002) - F*orest biomass estimation using polarimetric SAR interferometry.* Proceedings of the IEEE International Geoscience and Remote Sensing Symposium, pp. 817-819. doi: http://dx.doi.org/10.1109/IGARSS.2002.1025695.

Muukkonen P., Heiskanen J. (2005) - *Estimating biomass for boreal forests using ASTER satellite data combined with standwise forest inventory data.* Remote Sensing of Environment, 99 (4): 434-447. doi: http://dx.doi.org/10.1016/j.rse.2005.09.011.

Næsset E. (2011) - *Estimating above-ground biomass in young forests with airborne laser scanning*. International Journal of Remote Sensing, 32 (2): 473-501. doi: http://dx.doi.org/10.1080/01431160903474970.

Otsu N. (1979) - *A Threshold Selection Method from Gray-Level Histograms*. IEEE Transaction on Systems, Man and Cybernetics, 9 (1): 62-66. doi: http://dx.doi.org/10.1109/TSMC.1979.4310076.

Pan Y., Birdsey R., Phillips O.L., Jackson R.B. (2013) - *The Structure, Distribution, and Biomass of the World's Forests*. Annual Review of Ecology, Evolution, and Systematics, 44: 593-622. doi: http://dx.doi.org/10.1146/annurev-ecolsys-110512-135914.

Persson Å., Holmgren J., Söderman U. (2002) - *Detecting and measuring individual trees using an airborne laser scanner*. Photogrammetric Engineering And Remote Sensing 68 (9): 925-932.

Piqué M., Obon B., Condés S., Saura S. (2011) - *Comparison of relascope and fixed-radius plots for the estimation of forest stand variables in northeast Spain: An inventory simulation approach.* European Journal of Forest Research, 130 (5): 851-859. doi: http://dx.doi.org/10.1007/s10342-010-0477-x.

Popescu S.C., Wynne R.H., Nelson R.F. (2003) - *Measuring individual tree crown diameter with lidar and assessing its influence on estimating forest volume and biomass*. Canadian Journal of Remote Sensing, 29 (5): 564-577. doi: http://dx.doi.org/10.5589/m03-027.

R Development Core Team (2008) - *R: A Language and Environment for Statistical Computing*. R Foundation for Statistical Computing, Vienna, Austria. Available on line at: http://www.R-project.org.

Reitberger J., Schnörr C., Krzystek P., Stilla U. (2009) - *3D segmentation of single trees exploiting full waveform LIDAR data.* ISPRS Journal of Photogrammetry and Remote Sensing, 64 (664): 561-574. doi: http://dx.doi.org/10.1016/j.isprsjprs.2009.04.002.

Scrinzi G., Galvagni D., Marzullo L. (2010) - *I nuovi modelli dendrometrici per la stima delle masse assestamentali in Provincia di Trento.* Provincia Autonoma di Trento - Servizio Foreste e Fauna, Trento.

Tochon G., Féret J.B., Valero S., Martin R.E., Knapp D.E., Salembier P., Chanussot J., Asner G.P. (2015) - *On the use of binary partition trees for the tree crown segmentation of tropical rainforest hyperspectral images*. Remote Sensing of Environment, 159: 318-331. doi: http://dx.doi.org/10.1016/j.rse.2014.12.020.

Tonolli S., Dalponte M., Neteler M., Rodeghiero M., Vescovo L., Gianelle D. (2011) - *Fusion of airborne LiDAR and satellite multispectral data for the estimation of timber volume in the Southern Alps*. Remote Sensing of Environment, 115: 2486-2498. doi: http://dx.doi.org/10.1016/j.rse.2011.05.009.

Vaglio Laurin G., Chen Q., Lindsell J., Coomes D., Frate F. Del Guerriero L., Pirotti F., Valentini R. (2014) - *Above ground biomass estimation in an African tropical forest with lidar and hyperspectral data*. ISPRS Journal of Photogrammetry and Remote Sensing, 89: 49-58. doi: http://dx.doi.org/10.1016/j.isprsjprs.2014.01.001.

Vastaranta M., Holopainen M., Haapanen R., Yu X., Melkas T. (2009) - *Comparison Between an Area-Based and Individual Tree Detection Method for Low-Pulse Density ALS-Based Forest Inventory*. International archives of photogrammetry and remote sensing and spatial Information Sciences, 38: 147-151.

Vauhkonen J., Ene L., Gupta S., Heinzel J., Holmgren J., Pitkänen J., Solberg S., Wang Y., Weinacker H., Hauglin K.M., Lien V., Packalén P., Gobakken T., Koch B., Næsset E., Tokola T., Maltamo M. (2012) - *Comparative testing of single-tree detection algorithms under different types of forest*. Forestry, 85: 27-40. doi: http://dx.doi.org/10.1093/forestry/cpr051.

Yu X., Hyyppä J., Holopainen M., Vastaranta M. (2010) - *Comparison of area-based and individual tree-based methods for predicting plot-level forest attributes*. Remote Sensing, 2 (6): 1481-1495. doi: http://dx.doi.org/10.3390/rs2061481.